Supplementary Data for NAR-01480-D-2023

Structure-specific roles for PolG2-DNA complexes in maintenance and replication of mitochondrial DNA

Jessica L. Wojtaszek, Kirsten E. Hoff, Matthew J. Longley, Parminder Kaur, Sara N. Andres, Hong Wang, R. Scott Williams, and William C. Copeland

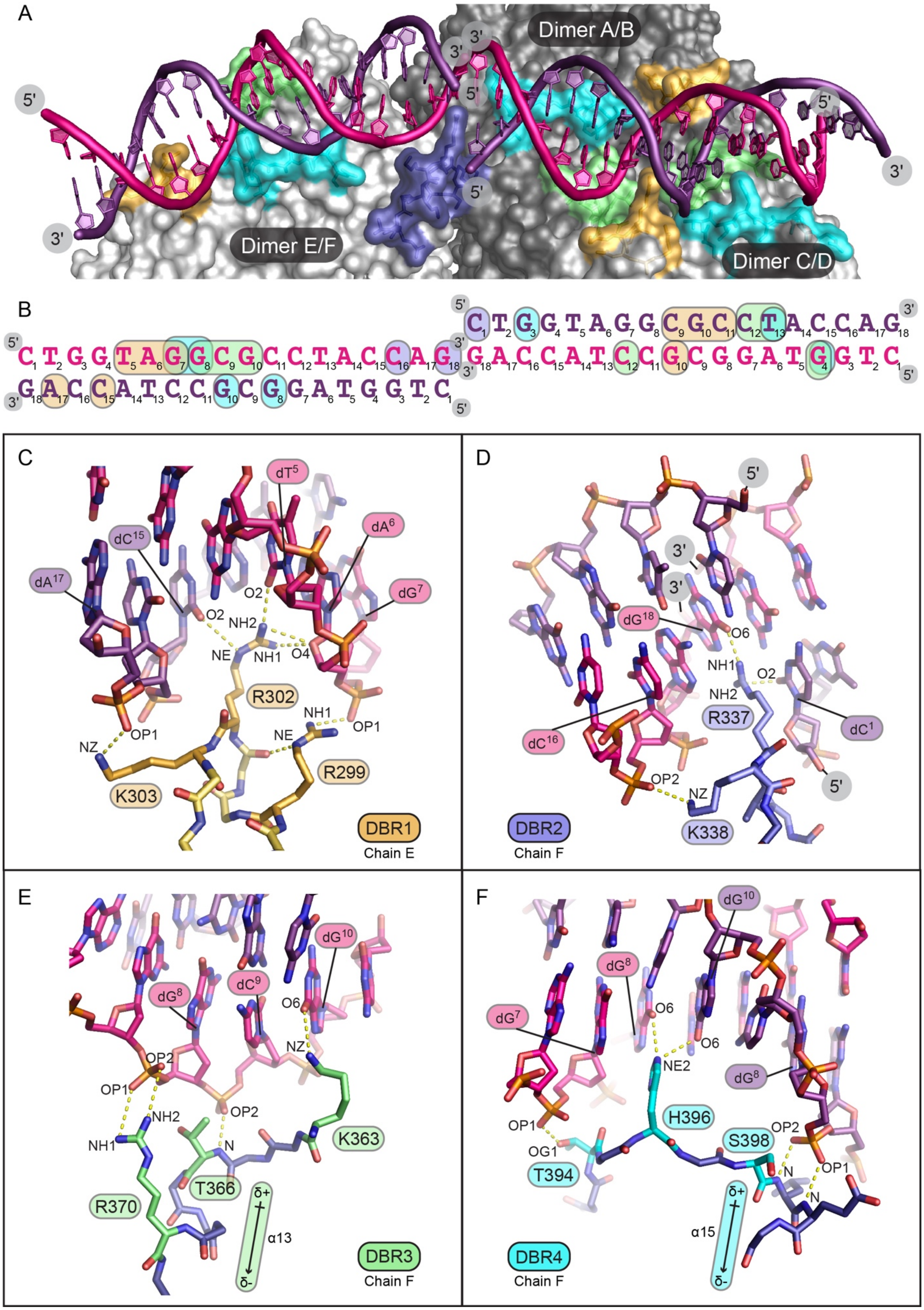

A
5'
3'
Dimer A/B
Dimer E/F
Dimer C/D
B
5' CTGGTAGGCGCCTACCAG 3'
5' CTGGTAGGCGCCTACCAG 3'
3' GACCATCCGCGGATGGTC 5'
3' GACCATCCGCGGATGGTC 5'
C
dT5
dA6
dG7
dC15
dA17
O2
NH2
NE
NH1
O4
R302
NH1
OP1
NE
NZ
OP1
K303
R299
DBR1
Chain E
D
5'
3'
dG18
O6
NH1
O2
NH2
R337
dC16
dC1
OP2
NZ
K338
DBR2
Chain F
E
dG10
dG8
dC9
O6
NZ
OP2
OP1
NH2
OP2
NH1
N
K363
T366
R370
δ+
δ-
α13
DBR3
Chain F
F
dG10
dG8
dG7
O6
O6
NE2
dG8
H396
OP1
OG1
T394
S398
OP2
N
OP1
N
δ+
δ-
α15
DBR4
Chain F

Figure S1. The DNA-PolG2 hexamer DBR interactions in detail.
A – All DBRs interacting with the two dsDNA molecules on the same contiguous surface of one face of the hexamer are shown in color: DBR1 in gold, DBR2 in deep blue, DBR3 in lime green, DBR4 in cyan. Dimer E/F alone engages the first dsDNA molecule while both Dimer A/B and Dimer C/D engage the second dsDNA molecule.
B – Diagram of the two 18-mer palindromic dsDNA molecules in the PolG2 hexamer structure. Protein-DNA interactions are labeled by encircling affected nucleotides consistent with coloring of DBRs1-4. Note that several DBRs 1, 3 and 4 from different chains interact with the dsDNA molecules but only one DBR2 (from Chain F on this face of the hexamer) engages the central 3'-3' join of the two dsDNA molecules. Also, although only one PolG2 dimer engages the first dsDNA vs two dimers engaging the second, nearly the same number of interactions is made to each dsDNA.
C – Chain E DBR1 in detail reveals R302sc making hydrogen bonds to the oxygens of bases dC^{15} and dT^{5} and sugar of dA^{6} within the minor groove. R299sc and K303sc make hydrogen bonds to backbone phosphate oxygens.
D – Chain F DBR2 in detail reveals R337sc base stacking with 5' terminal dC^{1} of the second dsDNA molecule whilst also hydrogen bonding to the base of 3' dG^{18} of the first dsDNA molecule. K338sc is hydrogen bonding to the phosphate oxygen of dC^{16}.
E – Chain F DBR3 in detail reveals major groove contacts with R370sc hydrogen bonding to the phosphate oxygens of dG^{8} and K363sc to the base of dG^{10}. T366sc packs against the sugar of dG^{8} whilst its backbone nitrogen hydrogen bonds to the phosphate oxygen of dC^{9} at the positive top of the α13 helix dipole.
F – Chain F DBR4 in detail reveals major groove contacts with H396sc hydrogen bonding to the bases of dG^{8} and dG^{10} and T394sc hydrogen bonding with the backbone phosphate oxygen of dG^{7}. S398sc serves as a helix cap for α15 whose dipole moment allows the backbone nitrogens of L399 and E400 at the positive start of the helix to hydrogen bond to the backbone phosphate oxygens of dG^{8}.

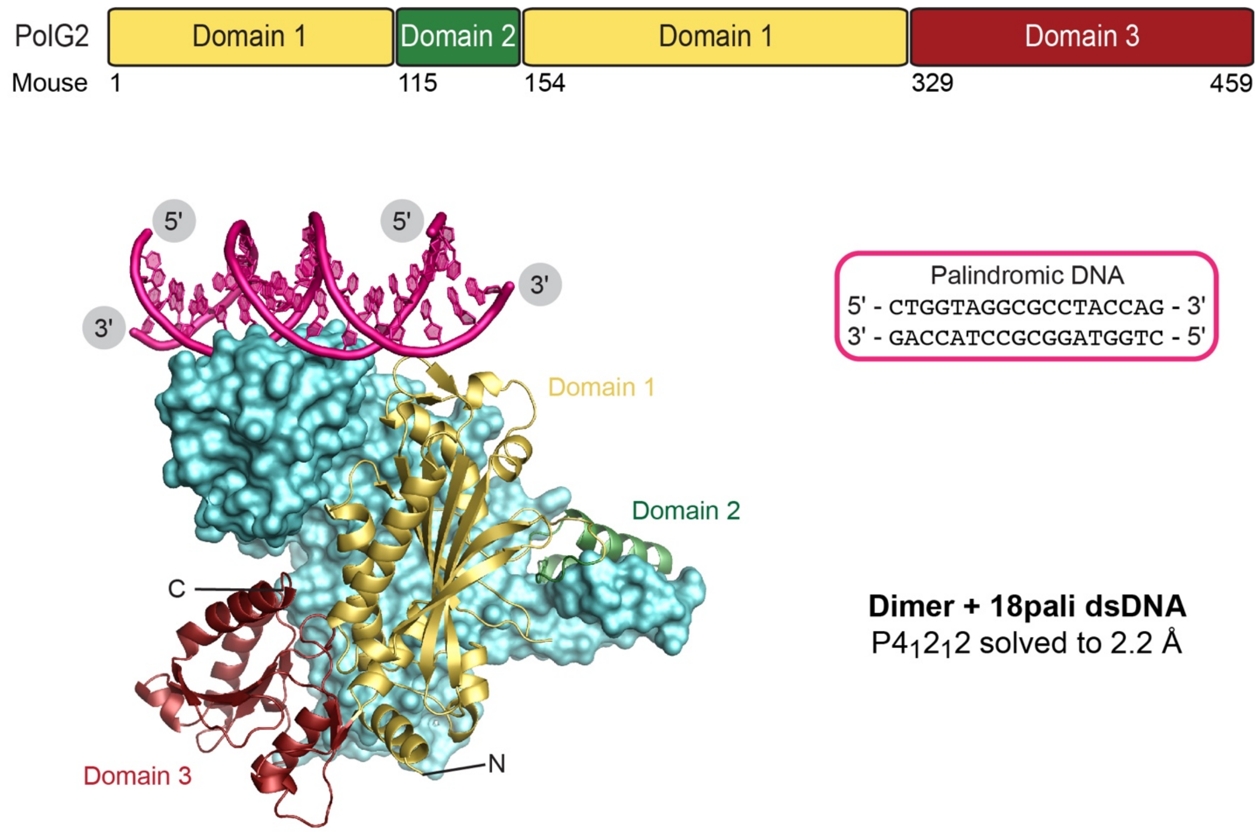

Figure S2. The DNA-PolG2 dimer crystal structure. The asymmetric unit of the dimer crystal is made up of two chains of mouse PolG2 and one palindromic dsDNA shown in hot pink.

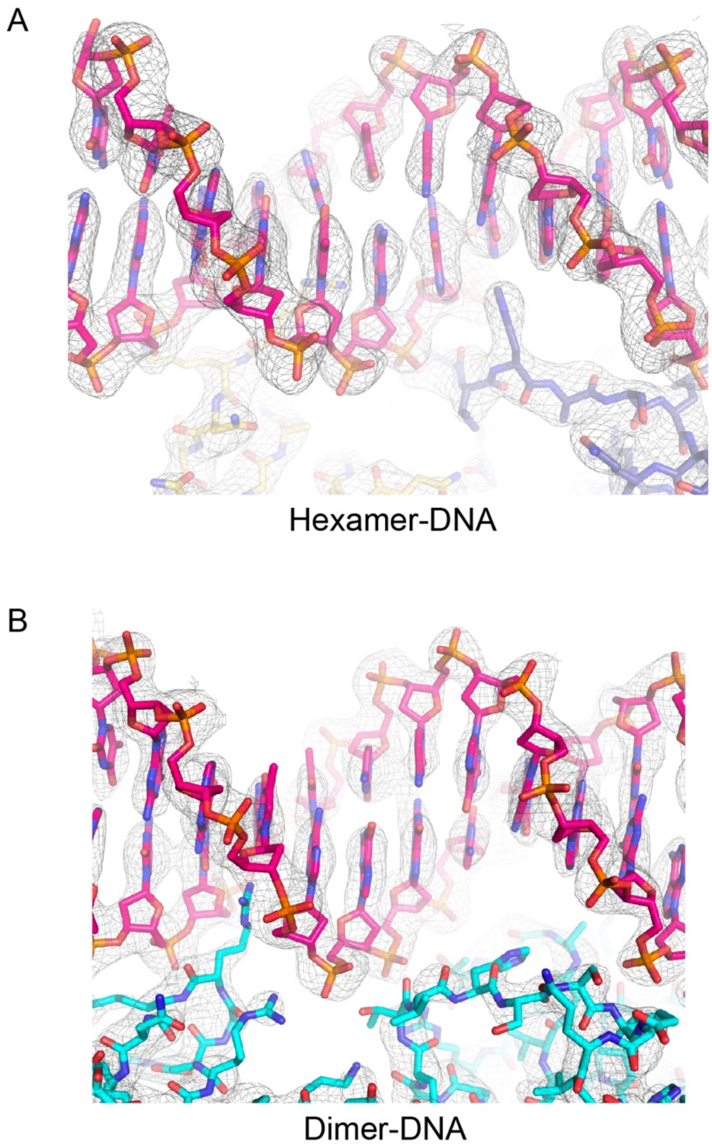

Figure S3. Representative composite annealed omit maps of the (A) PolG2 Hexamer-DNA and (B) PolG2 Dimer-DNA crystals.

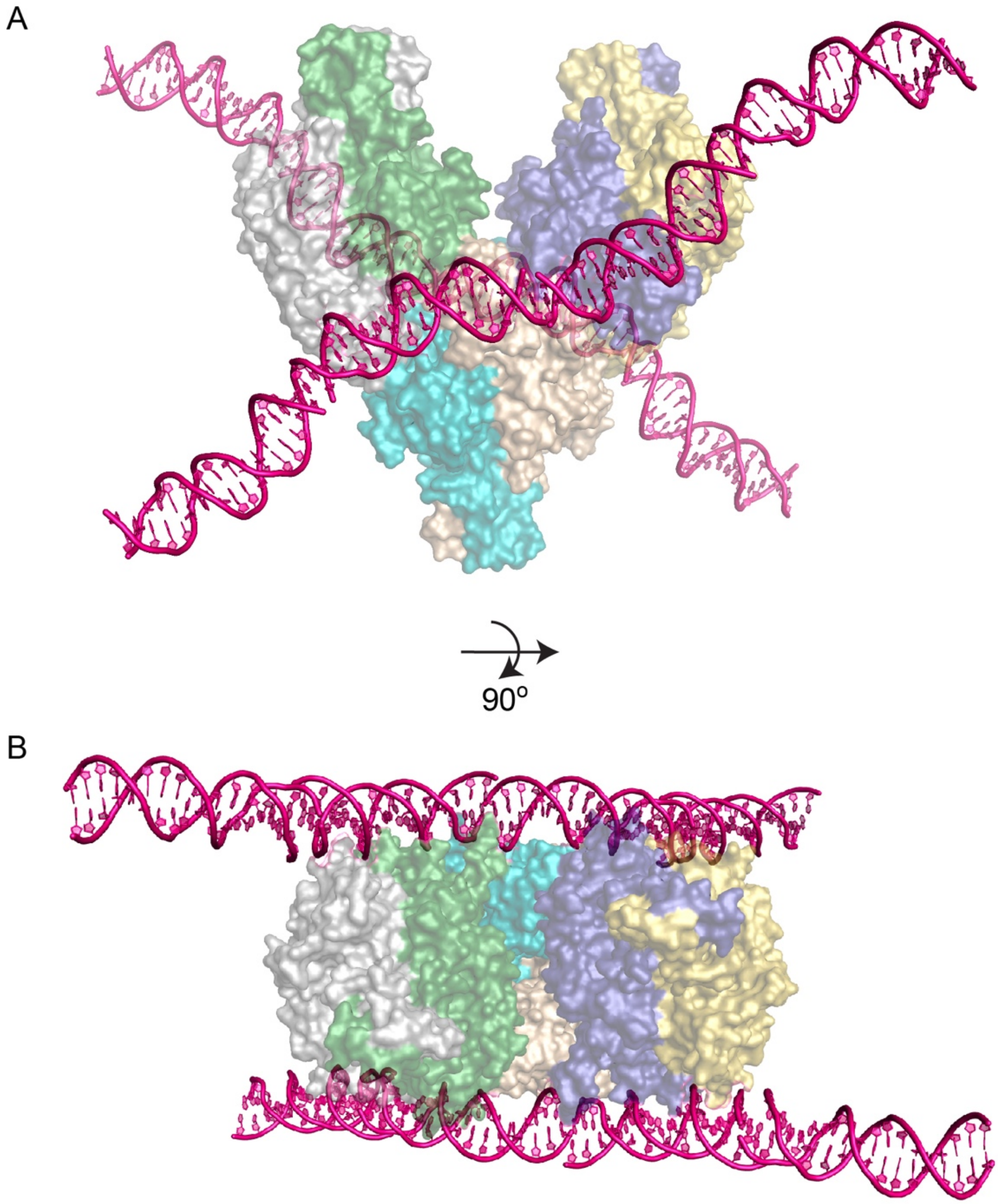

Figure S4. The PolG2 hexamer binds DNA on two sides to form crisscrossed DNA structures also observed in AFM.

A – DNA from symmetry related molecules within the crystal lattice are shown.

B – The orthogonal view of A clearly shows equivalent and symmetrical DNA binding on both sides of the PolG2 hexamer within the crystal.

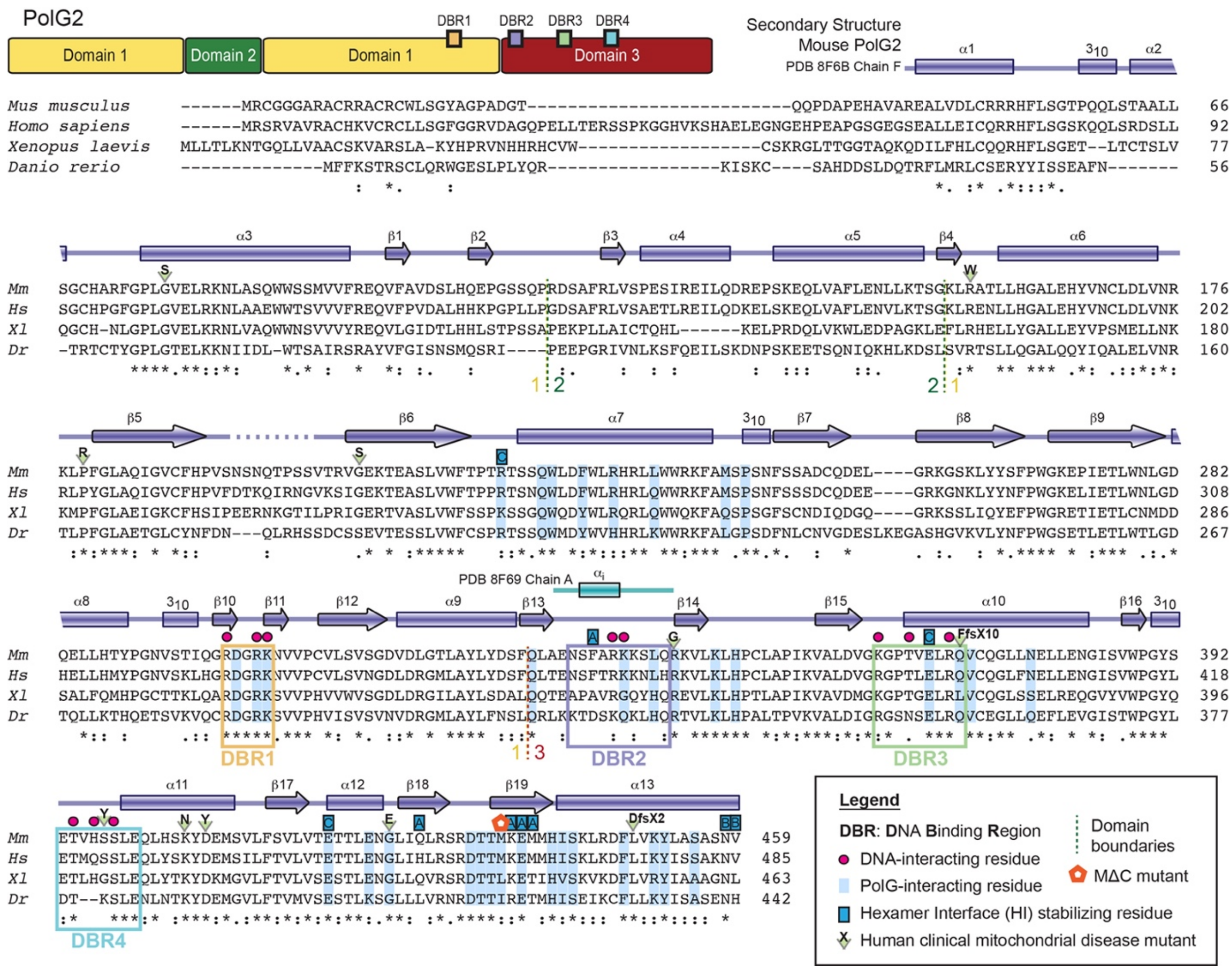

Figure S5. Sequence alignment of PolG2 made with Clustal W. The secondary structure represents Chain F of the hexamer. PolG-interacting residues are indicated from structure PDB 4ZTU. Select human clinical disease variants from ClinVar (NCBI) and gnomAD (Broad Institute) are indicated.

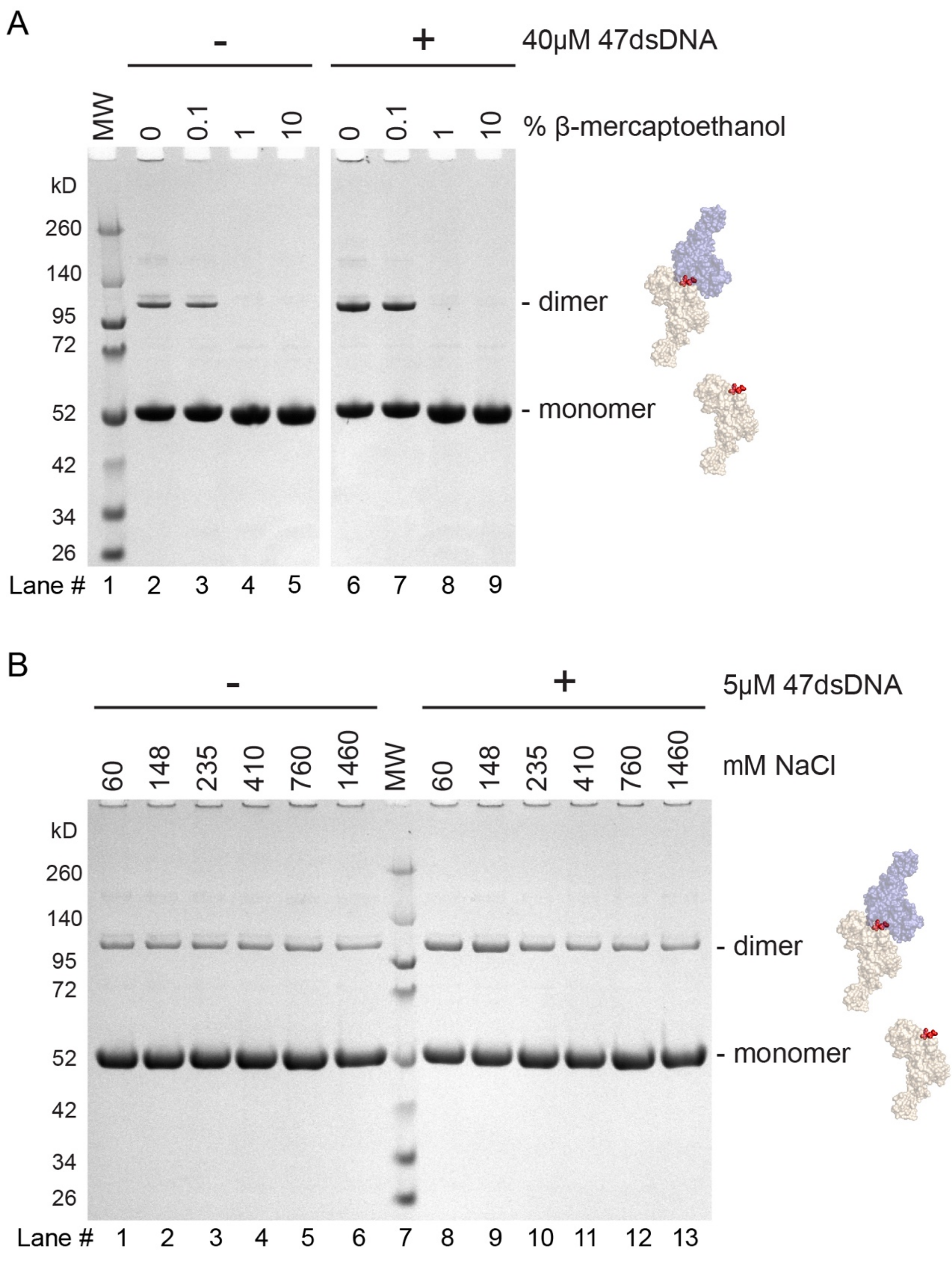

Figure S6. The engineered disulfide is reversible and the DNA-stimulation is salt sensitive.
A – Denaturing SDS-PAGE with varied reducing conditions indicates the M462C human PolG2 disulfide-dimer formation is reversible with the addition of 2-mercaptoethanol.
B – Non-reducing denaturing SDS-PAGE shows that formation of the DNA-stimulated M462C human PolG2 disulfide-dimer is salt sensitive.

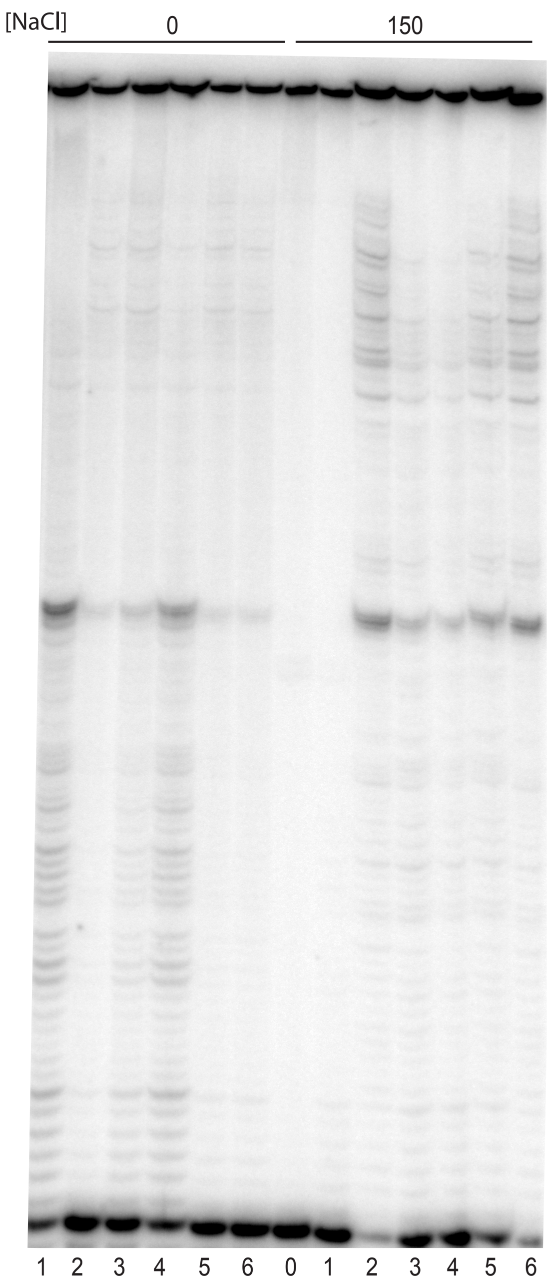

Fig S7. Urea-Polyacrylamide gel of the primer extension assay with PolG and the WT and DBR mutants of PolG2. Reactions contained either no added salt or 150 mM NaCl as indicated at the top of the gel. Reactions contained either no enzyme (lane 0) or PolG (lanes 1-6) with WT PolG2 (lane 2), DRB1-Ala PolG2 (lane 3), DRB2-Ala PolG2 (lane 4), DRB3-Ala PolG2 (lane 5), or DRB4-Ala PolG2 (lane 6), as described in the Methods and Materials.

Table S1. Table of X-ray Data Collection and Refinement Statistics

	PolG2 Dimer and 18pali DNA	**PolG2 Hexamer and 18pali DNA**
Wavelength (Å)	1.000	1.000
Resolution range (Å)	42.633 - 2.202 (2.281 - 2.202)	36.41 - 2.747 (2.845 - 2.747)
Space Group	P 41 21 2	P 32
Unit cell	88.027 88.027 343.17 90 90 90	116.224 116.224 250.938 90 90 120
Unique reflections	69448 (6754)	98448 (9883)
Multiplicity	8.9 (8.7)	2.9 (2.9)
Completeness (%)	99.69 (99.16)	99.81 (99.99)
Mean I/sigma (I)	20.59 (1.10)	18.96 (1.08)
Wilson B-factor	59.35	82.15
R-meas	0.127 (1.49)	0.096 (1.006)
R-pim	0.044 (0.494)	0.056 (0.583)
CC1/2	(0.606)	(0.488)
R-work	0.1939 (0.3305)	0.1960 (0.3003)
R-free	0.2283 (0.3417)	0.2216 (0.3636)
RMS (bonds)	0.004	0.002
RMS (angles)	0.64	0.43
Ramachandran favored (%)	97.39	96.99
Ramachandran outliers (%)	0.00	0.00
Average B-factor	83.91	96.99
macromolecules	84.02	96.51
ligands	95.88	98.49
solvent	70.16	81.45

Statistics for the highest-resolution shell are shown in parentheses.

Table S2. Structural analysis of selected human PolG2 mitochondrial disease variants

Mutation		Clinical Significance and Phenotype (from NCBI ClinVar and Broad gnomAD)	Structural Significance	References (PMID)
Human	Mouse			
G103S	G77S	Conflicting interpretations of pathogenicity – condition not provided	Internal residue of Domain 1 May affect protein packing/folding	21555342
R182W	R156W	Likely pathogenic – Mitochondrial DNA depletion syndrome 16A, Acute liver failure	Located at dimer interface, likely distorts interface or exposed hydrophobic W affects folding	30157269 27592148
P205R	P179R	Pathogenic - Progressive external ophthalmoplegia with mitochondrial DNA deletions, autosomal dominant 4	Position and charge could affect distal PolG2-PolG interaction, proximal PolG2 interaction with PolG AID domain, and HI-C	21555342
G232S	G206S	Conflicting interpretations of pathogenicity – Hereditary spastic paraplegia	Located at the dimer interface but the serine sidechain would likely point internally – may affect packing and distort interface	31286721
R369G	R343G	Conflicting interpretations of pathogenicity - Progressive external ophthalmoplegia with mitochondrial DNA deletions, Hereditary spastic paraplegia	Destabilizes extended DBR2 with expectation of affecting DNA-binding and hexamerization	21555342 22155748 22176657 23197651 23596069 26123486 26251896 27535533
Q397F fsX10	Q371F fsX10	Pathogenic – condition not provided	Truncates protein after DBR3 – loss of C-terminus removes DBR4, Hexamer Interfaces, and PolG interactions	28078310 29625556
S423Y	S397Y	Conflicting interpretations of pathogenicity – condition not provided	Located in DBR4, sidechain points internally, likely distorts loop	21555342 27065468
K431N	K405N	Likely pathogenic – condition not provided	K forms salt bridge with human E419 (mouse E393) – N may not form salt bridge, destabilizing fold	

D433Y	D407Y	Pathogenic - Mitochondrial DNA depletion syndrome 16B (neuro-ophthalmic type)	D forms salt bridges with human R456 and R369 (mouse R430 and R343) – Y disrupts charge interactions, destabilizing fold	31778857
G451E	G425E	Pathogenic - Progressive external ophthalmoplegia with mitochondrial DNA deletions, autosomal dominant 4	Involved in both proximal and distal PolG2-PolG interaction – E may disrupt transition from helix to strand	21555342 16685652
L475D fsX2	L449D fsX2	Pathogenic - Progressive external ophthalmoplegia with mitochondrial DNA deletions, autosomal dominant 4	Truncation removes HI-B and three PolG interacting residues	21555342

Predictions of structural significance are based on our structures of murine PolG2 dimers (PDB 8F69) and hexamers (PDB 8F6B), as well as the architecture of the human PolG-PolG2-DNA ternary complex (PDB 4ZTU).